

Dear editor,

Please see below the point by point work based on the 2 referees comments. Major changes include enlargement of the section about tectonic and stratigraphic setting to address main concerns by referee 2; re-structuring of the sections to include a "Results and discussion" section divided into 4 subsections to discuss more focused and substantially the modeling results (including limitations of the assumptions), correlation of modeled stresses with structural features, seepage evolution coupled to tectonic stress variations, and the potential effect of additional stress sources (e.g., from glacial isostasy) mainly on past seepage. We included results on the orientation of the principal modelled stress and discuss the implications of favorably oriented stresses with respect to existing faults in terms of opening for fluids. We added one figure to support the description of the faults and correlation between fault orientation and orientation of modelled tectonic stresses. The figure showing the modeled stresses was updated with the projection of the stress vectors.

We believe the manuscript has been considerably improved we look forward to yours and the referees opinion.

Point by point response to referee 1:

-Authors consider that only spreading centers are relevant and propose to use Okada's elastic solution for dislocations in an infinite elastic space to model the stress generated by the two spreading centers they are interested in. Interestingly they place the spreading centers below the brittle-ductile transition and assume a 7 mm/y opening rate. Hence, not only they use an elastic solution for analyzing the opening of a dislocation in the ductile part of the lithosphere, but they assume symmetry for the velocity of plates on both sides of the ridge, a feature which ought to be discussed.

We modified the text in places to clearly describe the limitations and strengths of implementing the Okada's solutions and provide arguments for why despite the limitations of the model simplicity and assumptions, the results are a realistic first order representation of tectonic stresses in the region. We extended on the symmetry assumption and indicated that this question may be better addressed after the acquisition of new aeromagnetic data on the west-Svalbard margin.

-Finally they consider that the pore pressure associated with the seepage of methane is larger than the minimum principal stress in the rock formation. But when pore fluid pressure is larger than the minimum principal stress, a hydraulic fracture is formed that keeps propagating till the pressure is released and becomes smaller than the minimum principal stress. This should have been discussed.

We restructured the discussion section. We included some statements indicating that mechanisms as hydro fracturing are indeed important modulators of the pore fluid pressure and dynamic behavior of the system. A couple of new references have been added to the discussion.

-I personally completely disagree with authors proposition that the glacial rebound does not affect presently the stress field and is negligible as compared to the effect of the spreading centers. In addition topography effects are most likely significant and the appropriateness of neglecting them should be demonstrated. Independently, because of the above mentioned difficulties concerning the proposed model : 1) with using Okada's elastic solution for modeling the stress field generated by a dislocation in a ductile material, 2) by assuming symmetry of plate motions on both sides of the ridge, 3) by considering that hydraulic fractures may remain stable for long durations of time, I cannot accept the paper as is. I propose a complete revision that will include a discussion showing why all my comments here above are irrelevant.

Regarding point one and two, we emphasize that the Okada model does, admittedly, involve simplifying assumptions that may not be necessarily perfectly fitting the structural setting in the region. We argue however that the model approach has been implemented for other margins where GPS has been used to validate the results. For example, Árnadóttir et al. (2009). The predicted stress directions from Okada models are in general agreement with other models of plate tectonic forces (for example, Bott, 1991; Gölke & Coblenz, 1996; Fejerskov & Lindholm, 2000; Naliboff et al., 2012). The good agreement between the predicted stress field and the observed focal mechanisms, furthermore, indicate that the model correctly predicts the first order stress field at upper crustal depths (as mentioned above). All these is conveyed in the main text.

For 2 and 3 please see above.

-In lines 110 to 113 of authors paper, it is written: "Because the model only incorporates plate spreading, it is likely that the actual stress field on the west-Svalbard margin differs to some extent from the stress field predicted by our model. However, by excluding all other sources of stress, we are able to investigate the influence of tectonic stress exclusively." I consider this statement demonstrates an error of judgement: the ongoing methane seepage depends on the coupling between fluid pressure and the presently existing complete stress field, as explained here after.

On line 114, authors state that they use Okada model of dislocations for modeling what they call tectonic stresses. This assumes elasticity. In elasticity, if four different loading processes are considered, the superposition of all of them at the same time implies that the resulting stress field may be evaluated from the sum of the four stress fields computed independently for each of the loading processes. Authors have listed as loading mechanisms: A ridge opening, B topography, C effect of sediment erosion-deposition, D flexural stresses due to glaciation. Hence, according to authors, present stress field result from A+B+C+D. Claiming that it can be investigated by looking at A only, implies that B+C+D are negligible. This requires a demonstration! Nowhere have I seen in the paper computations for B, C, and D.

We modified the paper in several places to make clear that the study intends to report on an important qualitative observation that forms the basis for understanding the interaction between regional processes and near-surface fluid dynamics in Arctic settings. We hope that it appears clear now that the modelled stresses cannot be considered a quantitative representations of total stresses in the region because we only investigate the kind of stresses potentially generated by oblique spreading and how these would affect existing faults and associated fluid migration. We elaborated on the arguments for considering the tectonic stresses to be dominant in this study area. We also added arguments for why glacial isostasy at present is not likely to be more dominant than the spreading stress but that it is likely that in the past these stresses were more significant in the region (providing an additional source of stress for explaining seepage in more extended areas along the Vestnesa Ridge).

-When I say "no reference is made to well documented on going glacial rebound", this is precisely what I mean. I do not mean authors have not cited previous work, I am saying they have not compared the magnitude of the glacial rebound effect to that of ridge opening at the location of methane seepage. As a reviewer of a scientific paper, I am careful to check facts, not speculations. I do not consider that authors response to my review do address properly the issue of quantifying effects B, C, and D.

Please see above

-I also do not wish to get involved into endless discussions on whether authors understand what is hydraulic fracturing or not, etc. : :I just did what I consider the work of a reviewer should be, i.e. check facts or validity of computations; I will leave the editor in chief decide whether my comments are relevant or not. I will stop here my time devoted to this paper and do not wish to be further involved in reviews for the journal "Solid Earth". Indeed, I am not interested in discussing opinions: : my small education just helps me with scientific demonstrations within my very small field of expertise...

We thank the reviewer for devoting time to review the paper and apologize for any misunderstandings.

Referee 2:

1. Structural setting of the Vestensa ridge. The structural setting of Vestensa ridge is of crucial importance for understanding active and relict seepage that has localized on this structure. However, description of structural geology is sloppy in many points. To start with, the manuscript misses a discussion regarding the possible genetic relationships between the Vestensa ridge and the Molloy/Knipovich oceanic ridges and their associated transform faults. In addition, origin, age and tectonic structure of the Vestensa ridge have not been discussed. The seismic section illustrated in figure 2 shows the geometry of a gentle anticline. I assume that this anticline corresponds to the Vestensa ridge, yet no location of this seismic section is reported. In addition, the Vestensa ridge shows a marked variation of its trend, with its western sector trending NW and the eastern sector oriented ca. NNW. Does this variation correspond to a difference in structural controls? Panel (b) of Figure 1 should be expanded conveniently to illustrate the location of active and extinct seeps, together with the trace of faults and the anticline axis shown in Figure 2.

We restructured section 2 to add substance to the description of the structural setting along the Vestensa Ridge,. We added a figure (new figure 2) to insert the main observations and descriptions from Plaza-Faverola et al., 2015 into this paper. We also use this figure to project the modeled orientation of stresses on imaged faults to analyze favorable orientation of principal stresses for creating opening along the structures (following the suggestion by referee 2).

2. Fold activity. As far as I can tell, the 'Vestensa' anticline deforms post-1.5 Ma Pleistocene sediments. A central point thus regards the establishment of whether the fold is still active or not. This point may be important in that anticlines are the preferential locus of active seepage because they trap the raising fluids at the fold core. Outer arc (extrados) normal faults may thus provide efficient fluid pathways. Many of the faults dipping toward the fold core (sketched on Figure 2 seismic section) could belong to this category. The amplification of this fold would thus be accommodated by the formation of new faults and/or the opening of existing ones. This possibility could be relevant in case this fold has been controlling active seepage. Again, this calls upon the requirement for a better definition of the structural setting of the Vestensa ridge (point above).

As part of the restructuring of section 2, we also elaborated/clarified that the Vetsnesa ridge is a contourite drift and its development as an anticline feature is strongly controlled by bottom currents (i.e., it has a sedimentological origin). We indicated relevant references. We also put more emphasis on the fact that even if the ridge is not a structural anticline its crest is the focus of fluids migrating toward the highest point of the ridge. We inserted in figure 2, insets from 2 seismic crosslines from Bünz et al and Johnson et al showing the variation on the morphology of the ridge on the western and eastern segments respectively.

3. Geometric relationships between stress field and pre-existing faults. A interesting point suggested by the modelling results is that existing normal faults could be opened by the operating tensile stress. Normal faults experience sealing-opening cycles that are typically dictated by fluid pressure pulses. On the other hand, this behavior is also controlled by the geometric relationships between the orientation of stress axes and the pre-existing structures. One can note in Figure 3 that active seepage occurs along a NW-trend, whereas inactive seeps occur along a ca. E-W trend. I wonder whether active seepage is depending upon the geometrical relationships between the orientation of regional stress field and the trend of faults. The distinction between active and relict seepage is essentially based on the assumption that a tensile stress regime favors seepage whereas a strike-slip one would not. This reasoning may be not invariably true because strike-slip faults are often steep and connect the subsurface reservoir to the surface, thereby representing efficient fluid pathways. As a matter of fact, there are many examples worldwide where active seepage focuses on both inactive and active strike-slip faults, as well as extensional jogs forming along strike-slip fault systems. In this regard, the manuscript should discuss more deeply why seepage along faults that fall into areas with strike-slip regime is discouraged. Is it because the maximum horizontal stress S_H is sub-orthogonal to fault trend? In case the maximum horizontal stress S_H is favorably oriented for reactivation, faulting would instead favor fluid upraising. This point could be resolved by showing the orientation of S_H and/or S_h axes throughout the study area, together with fault traces on the Vestensa ridge.

We followed the reviewer suggestion (as mentioned above) and included in the new figure 2 the projection of the stresses from the modeling figure which now includes the vectors from maximum horizontal compressive stresses as well in the entire modeling area. The geometric relationship between the modeled stresses and preexisting faults should appear clearer now. We clarify that a favorable orientation of the principal stresses can indeed favor opening of faults in the strike slip regime as well. The discussion about seepage coupled to stress field variations and pore fluid pressure interactions has been substantially improved.

4. Earthquake-induced seepage. It is assumed that (line 61) 'Our study is in line with observations of earthquake-induced seafloor seepage'. However, it should be noted that seepage and/or paroxysmal activity is not necessarily linked to earthquakes, but generally result from the 'normal' evolution of the system. Earthquakes represent obvious external forcing that may occasionally interfere with the system.

This sentence and paragraph in the introduction has been reformulated.

Sincerely,

Andreia Plaza-Faverola and Marie Keiding

CORRELATION BETWEEN TECTONIC STRESS REGIMES AND METHANE SEEPAGE ON THE WEST-SVALBARD MARGIN

A. Plaza-Faverola¹ and M. Keiding²

¹ CAGE-Centre for Arctic Gas Hydrate, Environment, and Climate; Department of Geosciences, UiT The Arctic University of Norway, N-9037 Tromsø, Norway

² Geological Survey of Norway (NGU), P.O. Box 6315 Torgarden, 7491 Trondheim, Norway

Correspondence to: Andreia Plaza-Faverola (Andreia.a.faverola@uit.no)

Abstract. Methane seepage occurs across the west-Svalbard margin at water depths ranging from the upper shelf at < 300 m to gas hydrate systems in the deep sea at > 1000 m. The Vestnesa sedimentary ridge, partially located on oceanic crust at 1000-1700 m water depth, hosts a perennial gas hydrate and associated free gas system. Present day seepage activity is restricted to the eastern segment of the sedimentary ridge, despite morphological and paleontological evidence for past seepage activity along the entire ridge extent. On the ridge, an eastward transition from ~~a-the~~ zone with clear morphological evidence of past seepage to ~~a-the~~ zone of active present-day seepage coincides with a change in the faulting pattern of near-surface strata. We modelled the tectonic stress regime exclusively due to oblique spreading along the Molloy and Knipovich spreading ridges to investigate whether spatial and temporal variations in the ~~spreading-related stress field~~ spreading-related stress field may explain patterns of seepage distribution. The model reveals a zone of tensile stress that extends northward from the Knipovich Ridge and encompasses ~~a-the~~ zone ~~of where extensional faulting and associated active seepage concentrate on the eastern segment of the Vestnesa Ridge.~~ The seemingly inactive part of the ridge is presently located in a strike-slip regime. Our modelling results suggest that present-day seepage can be explained by opening of faults and fractures favourably oriented with respect to spreading-related principal stresses, where pore fluid pressure overcomes the horizontal stress. Multiple seepage events along the entire extent of the gas-charged Vestnesa Ridge, may have been incited by favourably oriented mid-ocean ridge derived-stresses in the past or by additional sources of stress related for example to glacial isostasy. Our study provides a first order assessment of how stresses from mid-ocean ridge spreading may be influencing the kinematics of near-surface faults and associated seepage activity offshore the west-Svalbard passive margin.

1. INTRODUCTION

31 Seafloor seepage is a wide-spread phenomenon which consists in the release of natural gases into the oceans.
32 Hundreds of gigatonnes of carbon are stored as gas hydrates and shallow gas reservoirs in continental margins (e.g.,
33 Hunter et al., 2013). The release of these carbons over geological time is an important component of the global
34 carbon cycle. Understanding and quantifying seepage has important implications for ocean acidification, deep-sea
35 ecology and global climate. Periods of massive methane release from gas hydrate systems (e.g., Dickens, 2011) or
36 from large volcanic basins like that in the mid-Norwegian Margin (e.g., Svensen et al., 2004) have been linked to
37 global warming events such as the Palaeocene-Eocene thermal maximum. We know that methane seepage has been
38 occurring for millions of years, but we have a poor understanding of what forces it.

39

40 Present day seepage is identified as acoustic flares in the water column commonly originating at seafloor
41 depressions, while authigenic carbonate mounds are used as indicators of longer-term seepage activity (e.g., Judd
42 and Hovland, 2009). Seepage at the theoretical upstream termination of the gas hydrate stability zone (GHSZ) (i.e.,
43 coinciding with the shelf edge) on different continental margins, has been explained by temperature driven gas-
44 hydrate dissociation (e.g., Skarke et al., 2014; Westbrook et al., 2009). On formerly glaciated margins, active
45 seepage is believed to be associated with pressure changes resulting from the retreat of the ice-sheet (e.g.,
46 Andreassen et al., 2017; Portnov et al., 2016). The effect of post-glaciation uplift on gas hydrate stability has been
47 recently suggested as an alternative explanation for seepage localized at the shelf break offshore west-Svalbard
48 (Wallmann et al., 2018)

49

50 Across the formerly glaciated west-Svalbard margin, active seepage extends beyond the shelf break and the region
51 formerly covered by ice. As a matter of fact, active seepage sites have been identified from inside Isfjorden (Roy
52 et al., 2014) to water depths of ~1200 m (Smith et al., 2014) where the Vestnesa Ridge hosts a perennially stable
53 gas hydrate system beyond the ice-sheet grounding line. The Vestnesa Ridge is a NW-SE oriented contourite
54 deposit located between the northward termination of the Knipovich ridge and the eastern flank of the Mollo
55 spreading ridge in the Fram Strait (Fig. 1). Seafloor pockmarks along the Vestnesa Ridge, first documented by
56 Vogt (1994), exist along the entire ridge. However, acoustic flares have been observed to originate exclusively at
57 large pockmarks located on the eastern part of the sedimentary ridge (Fig. 1,2). The presence of inactive pockmarks
58 adjacent to a zone of active seepage along the Vestnesa Ridge, raises the question what stopped previously active
59 seepage sites?

60

61 Plaza-Faverola et al., (2015) documented seismic differences in the orientation and type of faulting along the ridge
62 and showed a link between the distribution of gas chimneys and faults. They ~~postulated~~ that spatial and temporal
63 tectonic stress variations have a long-term effect on the spatial distribution of fault-related gas migration and
64 seepage evolution. The information about the present day ~~the~~ stress regime in the Fram Strait is limited to large
65 scale lithospheric density models (Schiffer et al., 2018) ~~and a limited number of poorly constrained stress vectors~~
66 from earthquake focal mechanisms (Heidbach et al., 2010). Here, we experiment with an approach that allows us
67 to approximate the orientation and type of stress regimes exclusively due to oblique spreading at Molloy and
68 Knipovich Ridges. We study, qualitatively, how stresses from mid-ocean ridge spreading alone may be influencing
69 modelled the tectonic stress regime due to mid-ocean ridge spreading at Molloy and Knipovich ridges in Fram
70 Strait, to test how spreading at these ridges influences the tectonic field the kinematics of ~~near-surface faults and~~
71 associated methane seepage activity along the Vestnesa Ridge.

72
73 ~~The tectonic model contributes with additional evidence of a correlation between regional stress regime and~~
74 ~~seepage patterns along the Vestnesa Ridge initially postulated based on seismic interpretation (Plaza Faverola et~~
75 ~~al., 2015). Our study is in line. The effect of regional stresses on fluid dynamics in the near-surface has implications~~
76 ~~for seepage systems globally.~~
77 The relationship between fault kinematics and fluid migration has been documented specially at accretionary
78 margins with where observations of earthquake-induced seafloor seepage has been monitored (e.g., Geersen et al.,
79 2016) and stress field variations ~~display~~ faults are found to sustain shallow gas accumulations and seepage (Plaza-
80 Faverola et al., 2016). With the present study we show, using an Arctic case, that seepage on passive continental
81 margins may be affected as well by the stress regime at the mid-ocean ridges, at accretionary margins suggesting
82 that the effect of regional stresses on fluid dynamics in the near surface has implications for seepage systems
83 globally.

84 85 **2. GEOLOGICAL STRUCTURAL AND STRATGRAPHIC SETTING OF THE VESTNESA** 86 **RIDGE SEEPAGE SYSTEM**

87 In Fram Strait, sedimentary basins are within tens of kilometres from ultra-slow spreading Arctic mid-ocean ridges
88 (Fig. 1). The opening of the Fram Strait was initiated 33 Ma ago and evolved as a result of slow spreading of the
89 Molloy and Knipovich Ridges (Engen et al., 2008). An important transpressional event deformed the sedimentary
90 sequences of western Svalbard, resulting in folds and thrustbelts, during the Paleocene-Eocene dextral movement
91 of Spitsbergen with respect to Greenland. Transpression stopped in the early Oligocene when the tectonic regime

92 became dominated by extension (Myhre and Eldholm, 1988). The circulation of deep water masses through Fram
93 Strait started during the Miocene, ca. 17-10 Ma ago (Ehlers and Jokat, 2009; Jakobsson et al., 2007), establishing
94 the environmental conditions for the evolution of bottom current-driven sedimentary drifts (Eiken and Hinz, 1993;
95 Johnson et al., 2015). It has been suggested that the opening of the northern Norwegian–Greenland Sea was
96 initiated by the northward propagation of the Knipovich ridge into the ancient Spitsbergen Shear Zone (SSZ) (Crane
97 et al., 1991). The NW–SE oriented Vestnesa sediment depocenter, extends for ca. 100 km off the west Svalbard
98 passive margin (Fig. 1b) and developed in the tectonically complex transition zone from oceanic to continental
99 crust. In addition, t

100
101 he effect of ice sheet dynamics on the west Svalbard margin has influenced the stratigraphy, and most likely the
102 morphology, of the Vestnesa Ridge and adjacent sedimentary basins. The sedimentary succession along the
103 Vestnesa Ridge is > 5 km thick in places and has been divided in three main stratigraphic units : the deepest
104 sequence, YP1, consists of synrift and post rift sediments deposited directly on oceanic crust; YP2 consists of
105 contourites; and YP3, corresponding to the onset of Pleistocene glaciations (ca. 2.7 Ma ago) , is a mix of
106 glaciomarine contourites and turbidites.

107
108 The continental crust beneath the western coast of Svalbard thins towards the Hornsund Fault zone (HFZ) indicating
109 extension following the opening of the Greenland Sea (Faleide et al., 1991). Late Miocene and Pliocene
110 sedimentation, driven by bottom currents, resulted in the formation of the ca. 100 km long Vestnesa Ridge between
111 the HFZ off west-Svalbard and oceanic crust highs at the eastern flank of the Molloy mid-ocean ridge (Eiken and
112 Hinz, 1993; Vogt et al., 1994). The sedimentary ridge is oriented parallel to the Molloy Transform Fault (MTF)
113 and its crest experiences a change in morphology from narrow on the eastern segment to expanded on the western
114 Vestnesa Ridge segments (Fig. 2). The exact location of the continental-ocean boundary remain somewhat
115 uncertain (Eldholm et al., 1987) but it is inferred to be nearby the transition from the eastern to the western segments
116 (Engen et al., 2008).

117
118 The total sedimentary thickness along the Vestnesa Ridge remains unconstrained. Based on one available regional
119 profile it can be inferred that the ridge is > 5 km thick in places (Eiken and Hinz, 1993). It has been divided into
120 three main stratigraphic units (Eiken and Hinz, 1993; Hustoft, 2009): the deepest sequence, YP1, consists of synrift
121 and post-rift sediments deposited directly on oceanic crust; YP2 consists of contourites; and YP3, corresponding
122 to the onset of Pleistocene glaciations (ca. 2.7 Ma ago) (Mattingsdal et al., 2014), is a mix of glaciomarine

123 contourites and turbidites. The effect of ice-sheet dynamics on the west-Svalbard margin (Knies et al., 2009; Patton
124 et al., 2016) has influenced the stratigraphy, and most likely the morphology, of the Vestnesa Ridge and adjacent
125 sedimentary basins. In this Arctic region, glaciations are believed to have started even earlier than 5 Ma ago. The
126 onset of local intensification of glaciations is inferred to have started ca. 2.7 Ma ago (e.g., Faleide et al., 1996;
127 Mattingsdal et al., 2014). Strong climatic fluctuations characterized by intercalating colder, intense glaciations with
128 warmer and longer interglacials, dominated the last ca. 1 Ma. (e.g., Jansen and Sjøholm, 1991; Jansen et al., 1990).
129
130 A set of N-S to NNE-SSE trending faults cut the recent strata at a narrow zone between the Vestnesa Ridge and
131 the northern termination of the KR (Fig 1). Due to their structural connection with the KR they are believed to
132 indicate ongoing northward propagation of the rift system . High resolution 3D seismic data collected on the eastern
133 Vestnesa Ridge segments revealed sub-seafloor NW-SE oriented faults (i.e., near-vertical and parallel to the
134 sedimentary ridge axis) that could be genetically associated with the outcropping faults (Plaza-Faverola et al.,
135 2015; Fig. 2). Comparison of similar high resolution 3D seismic data from the western Vestnesa Ridge segment
136 shows that the style of faulting pattern has been radically different from that of the eastern segment. Here, only
137 randomly oriented small fault segments are revealed in a nevertheless pockmarked Holocene strata (Fig. 2).
138 Gravimetric data also indicate an abrupt structural change to the west compared to the east of a N-S oriented fault
139 separating the ridge segments (Plaza-Faverola et al., 2015).

140
141 The gas hydrate system dynamics along the Vestnesa Ridge seems to be highly influenced by spatial variations in
142 the geothermal gradient and the gas composition (Plaza-Faverola et al., 2017). Thermogenic gas ~~is~~ accumulations
143 at the base of the GHSZ (Fig. 2) are structurally controlled (i.e., the gas migrates towards the crest of the
144 sedimentary drift) and part of this gas sustains present day seepage activity (Bünz et al., 2012; Knies et al., 2018;
145 Plaza-Faverola et al., 2017). ~~Seepage has been~~ Reservoir modelling shows that source rock deposited north of the
146 MTF has potentially started to generate thermogenic gas 6 Ma ago and that migrating fluids reached the Vestnesa
147 Ridge crest at the active seepage site ca. 2 Ma ago (Knies et al., 2018). It is suspected that seepage has been
148 occurring, episodically, at least since the onset of the Pleistocene glaciations c. 2.7 Ma ago leaving buried
149 pockmarks and authigenic carbonate crusts as footprint (Plaza-Faverola et al., 2015). Many transient seepage events
150 are suspected and one was dated to ca. 17.000 years based on the presence of a ~1000 years old methane-dependent
151 bivalve community possibly sustained by a gas pulse through a fault (Ambrose et al., 2015).

152 153 **3. SEISMIC DATA**

154 The description of faults and fluid flow related features along the Vestnesa Ridge is documented in Plaza-Faverola et al., 2015.
155 The description is based on two-3D high resolution seismic data sets acquired on the western and the eastern Vestnesa Ridge
156 segments respectively, and one 2D seismic line acquired along the entire Vestnesa Ridge extent (Fig. 2 this paper). These data
157 have been previously used for the investigation of BSR dynamics (Plaza-Faverola et al., 2017) and documentation of gas
158 chimneys and faults in the region (Petersen et al., 2010; Plaza-Faverola et al., 2015). The data were acquired on
159 board R/V Helmer Hanssen using the 3D P-Cable system (Planke et al., 2009). Final lateral resolution of the 3D
160 data sets is given by a bin size of 6.25x6.25 m² and the vertical resolution is > 3 m with a dominant frequency of
161 130 Hz. Details about acquisition and processing can be found in Petersen et al., 2010 and Plaza-Faverola et al.,
162 2015. For the 2D survey the dominant frequency was ~80 Hz resulting in a vertical resolution > 4.5 m (assumed
163 as $\lambda/4$ with an acoustic velocity in water of 1469 m/s given by CTD data; Plaza-Faverola et al., 2017).

164

165 **4. THE MODELING APPROACH**

166 Tectonic processes at plate margins have a major influence on regional stress patterns (Heidbach et al., 2010).
167 Given the proximity to the Molloy and Knipovich Ridges, we hypothesise that ridge push has a major control on
168 the regional, tectonic stress field at Vestnesa Ridge. Other stress sources of importance in the region are
169 gravitational stresses due to bathymetry/topography and subsurface density contrasts and flexural stresses due to
170 sediment erosion and deposition. During the Quaternary, the west-Svalbard margin has furthermore been affected
171 by glacially induced flexural stresses due to the glaciations ___ (e.g., Fjeldskaar and Amantov, 2017; Patton et al.,
172 2016). [Models of stresses induced by the Fennoscandian ice sheet](#) (Lund et al., 2009; Steffen et al., 2006) [indicate](#)
173 [that the glacially induced stress on the continental margin is close to zero at present-day.](#)

174

175 [This study deals exclusively with](#) tectonic stress due to ridge push. -We use the approach by Keiding et al. (2009)
176 based on the analytical solutions derived by Okada (1985), to model the plate motion and tectonic stress field due
177 to spreading along the Molloy and Knipovich Ridges. Because the model only incorporates plate spreading, [the](#)
178 [stresses- resulting from the models cannot be considered as a representation of the total stress field in the region.](#)
179 However, [the objective of this study is not to model the total stress field, rather, the focus is to investigate how](#)
180 [tectonic stress may influence seepage in the proximity of the two spreading ridges.](#) By excluding all other sources
181 of stress [in the modelling](#), we are able to investigate the -influence of [tectonic stressplate spreading](#) exclusively.

182

183 The Okada model and our derivation of the stress field from it is described in more detail in appendix A. The
184 Molloy and Knipovich Ridges are modelled as rectangular planes with opening and transform motion in a flat

185 Earth model with elastic, homogeneous, isotropic rheology. Each rectangular plane is defined by ten model
186 parameters used to approximate the location, geometry and deformation of the spreading ridges (Okada, 1985; see
187 supplement Table 1). The locations of the two spreading ridges were constrained from bathymetry maps (Fig. 3).
188 The two spreading ridges are assumed to have continuous, symmetric deformation below the brittle-ductile
189 transition, with a half spreading rate of 7 mm/yr and a spreading direction of N125°E, according to recent plate
190 motion models (DeMets et al., 2010). Because the spreading direction is not perpendicular to the trends of the
191 spreading ridges, this results in both opening and right-lateral motion; that is, oblique spreading on the Molloy and
192 Knipovich Ridges. The Molloy Transform Fault, which connects the two spreading ridges, trends N133°E, thus a
193 spreading direction of N125°E implies extension across the transform zone. We use a depth of 10 km for the brittle-
194 ductile transition and 900 km for the lower boundary of the deforming planes, to avoid boundary effects. For the
195 elastic rheology, we assume typical crustal values of Poisson's ratio = 0.25 and shear modulus = 30 GPa (Turcotte
196 and Schubert, 2002).

197 [Asymmetric spreading has been postulated for the Knipovich Ridge based on heat flow data](#) (Crane et al., 1991),
198 [and for other ultraslow spreading ridges based on magnetic data](#) (e.g., Gaina et al., 2015) [\(However, the evidence](#)
199 [for asymmetry along the KR remains inconclusive and debatable in terms, for example, of the relative speeds](#)
200 [suggested for the North American \(faster\) and the Eurasian \(slower\) plates](#) (Crane et al., 1991; Morgan, 1981; Vogt
201 et al., 1994). [This reflects that the currently available magnetic data from the west-Svalbard margin is not of a](#)
202 [quality that allows an assessment of possible asymmetry of the spreading in the Fram Strait](#) (Nasuti and Olesen,
203 2014). [Thus, symmetry is conveniently assumed for the purpose of the present study.](#)

204
205 We focus on the stress field in the upper part of the crust (where the GHSZ is) and characterise the stress regime
206 based on the relative magnitudes of the horizontal and vertical stresses. We refer to the stresses as σ_v (vertical
207 stress), σ_H (maximum horizontal stress) and σ_h (minimum horizontal stress), where compressive stress is positive
208 (Zoback and Zoback, 2002). A tensile stress regime ($\sigma_v > \sigma_H > \sigma_h$) favours the opening of steep faults that can
209 provide pathways for fluids. [Favourable orientation of stresses with respect to existent faults or pore fluid pressures](#)
210 [as high as lithostatic pressures are additional conditions for favouring opening](#) under compressive ($\sigma_H > \sigma_h > \sigma_v$)
211 and strike-slip ($\sigma_H > \sigma_v > \sigma_h$) regimes (e.g., Graults and Baleix, 1994).

214 4. RESULTS AND DISCUSSION

215 4.1 PREDICTED STRESS FIELDS DUE TO OBLIQUE SPREADING

216
217 The model predicts zones of tensile stress near the spreading ridges, and strike-slip at larger distance from the
218 ridges. An unexpected pattern arises near the Vestnesa Ridge due to the interference of the stress from the two
219 spreading ridges. A zone of tensile stress extends northward from the Knipovich Ridge, encompassing the eastern
220 part of the Vestnesa Ridge. The western Vestnesa Ridge, on the other hand, lies entirely in a zone of strike-slip
221 stress (Fig. 4).

222
223 Sensitivity tests for realistic variations in 1) mid-oceanic spreading, 2) depth of the brittle-ductile transition, and 3)
224 elastic moduli, show that the tensile stress zone covering the eastern Vestnesa Ridge is a robust feature of the
225 model, that is, variations in the parameters result in a change of the extent and shape of the tensile zone but the
226 zone remains in place (Supplementary material).

227
228
229 To investigate the geometric relationship between the predicted stress field and mapped faults, we calculate the
230 orientations of maximum compressive horizontal stress (Lund and Townend, 2007). The maximum horizontal
231 stresses (σ_{hc}) within the tensile regime approximately follow the orientation of the spreading axes (i.e., dominantly
232 NE-SW to N-S; Fig. 4). Spreading along the Molloy ridge causes NW-SE orientation of the maximum compressive
233 stress along most of the Vestnesa Ridge, except for the eastern segment where the influence of the Knipovich Ridge
234 results in a rotation of the stress towards E-W (Fig. 4). It is important to wear in mind that the minimum horizontal
235 compressive stresses (σ_h) would be exerted in a plane perpendicular to the vectors in figure 4.

236
237 The simplifying assumptions involved in the Okada models (e.g., continuous, symmetric deformation below the
238 brittle-ductile transition) implies that the resulting stresses are unconstrained to a certain degree. However, Árnadóttir
239 et al. (2009) demonstrated that the deformation field from the complex plate boundary in Iceland could be modelled using
240 Okada models. In addition, the predicted stress directions from Okada models are in general agreement with other models of
241 plate tectonic forces (e.g., Gölke & Coblentz, 1996; Naliboff et al., 2012). Furthermore, a comparison of the predicted stress
242 from plate spreading and observed earthquake focal mechanisms shows an excellent agreement, both with regards
243 to style and orientation of the focal mechanisms. The earthquake focal mechanisms are mostly normal along the
244 spreading ridges and strike-slip along the transform faults, and the focal mechanism pressure axes align nicely with
245 the predicted directions of maximum compressive stress (Fig. 4). The good agreement between Okada's and other

246 modelling approaches as well as between the resulting stresses and focal mechanisms in the area indicates two
247 things: 1. that the model, despite the simplicity of its assumptions, provides a correct first order prediction of the
248 stress field in the upper crust, and 2. that stress from plate spreading may indeed have a dominant control on the
249 stress field along the Vestnesa Ridge.

252 4.2 SPATIAL CORRELATION BETWEEN MODELLED TECTONIC STRESS REGIME, FAULTING 253 AND FLUID FLOW FEATURES

255 The zone of tensile stress on the eastern Vestnesa Ridge segment coincides with a zone of faulting and where all
256 the present day seepage is concentrated (Fig. ~~32~~, ~~43~~). The match between the extend of the modelled tensile zone
257 and the active pockmarks is not exact; active pockmarks exist a few kilometres westward from the termination of
258 the tensile zone (Fig. ~~43~~). However, the agreement is striking from a regional point of view, considering the
259 uncertainty of the model as illustrated by the sensitivity tests (Supplementary material). In the predicted tensile
260 zone towards the east of the Vestnesa Ridge, the sub-seabed faults are NW-SE oriented, near vertical and have a
261 gentle normal throw (< 10 m). Normal faulting or tensile opening of these faults would be enhanced by NW-SE
262 oriented maximum compressive stress, i.e., the orientation of stresses predicted by our model on the crest and at
263 the southern flank of the ridge until the transition to the tensile stress regime (Fig. 4). This implies that these faults
264 are currently under a regime that makes them favourably permeable for fluids (Fig. 2). Indeed, ~~They~~ ~~(These faults~~
265 are spatially linked to gas chimneys and active seepage (Bünz et al., 2012; Plaza-Faverola et al., 2015). Some of
266 the faults show thicker sediment thicknesses at the hanging wall, allowing identification of discrete periods of
267 normal faulting (Plaza-Faverola et al., 2015).

269 The character of the faults changes towards the western Vestnesa Ridge ~~and the~~ where the model predicts strike-
270 slip regime (Fig. 2). The density of faulting and seismic definition decreases westward (Fig. 2, ~~3~~, ~~54~~). In this part
271 of the ridge gas chimneys are narrower, stacked more vertically than active chimneys towards the east and it is
272 possible to recognise more faults reaching the present-day seafloor (Plaza-Faverola et al., 2015~~).~~ Here, the
273 orientation of σ_H (NW-SE) is oblique to the more WNW-ESE to W-E oriented fault segments (Fig. 2, 4), suggesting
274 that, with some exceptions, these structures are not favourably oriented for tensile opening (Fig. 2).

276 ~~The~~A cluster of larger scale N-S to NNW-SSE trending extensional faults ~~that~~ outcrop at the southern slope of the
277 Vestnesa Ridge (Fig. 1, 2), also ~~within~~ ~~coincides with~~ the zone of predicted tensile stress (Fig. 4, 3). In agreement
278 with our models, these extensional faults have been suggested to indicate the northward propagation of the
279 Knipovich Ridge rift system (Crane et al., 2001; Vanneste et al., 2005). However, it is likely that faulting along
280 this steep slope of the Vestnesa Ridge (Fig. 1) was partially induced ~~as well~~ by gravitational stress.

281
282 The striking correlation between predicted tectonic stress regime, faulting structures and current seepage ~~does, in~~
283 ~~fact, suggest~~ ~~suggests~~ that tectonic stress ~~resulting from complex oblique spreading in the region~~, has potentially a
284 major influence on the near-surface sedimentary deformation ~~and fluid dynamics~~. Hereafter, we discuss the
285 implications of the interaction between tectonic stresses and pore-fluid pressure for the evolution of gas seepage
286 along the Vestnesa Ridge.

288 **4.3 SEEPAGE COUPLED TO STRESS CYCLING**

289
290 Based on the correlation between tectonic stress regimes and seepage patterns, we postulate that current seepage at
291 the eastern Vestnesa Ridge segment is favoured by the opening of pre-existing faults in a tensile stress regime (Fig.
292 2, 3a). Depending on the tectonic regime, permeability through faults and fractures may be enhanced or inhibited
293 (e.g., Faulkner et al., 2010; Hillis, 2001; Sibson, 1994). Thus, spatial and temporal variations in the tectonic stress
294 regime may control the transient release of gas from the seafloor over geological time as documented, for example,
295 for CO₂ analogues in the Colorado Plateau (e.g., Jung et al., 2014).

296
297 ~~It is likely that the steep NW-SE oriented faults mapped along the eastern Vestnesa Ridge segment formed in a~~
298 ~~strike-slip regime and became permeable to fluids over time. We envision that seepage is induced 1) by opening of~~
299 ~~faults along, favourably oriented with respect to the stress field and 2) by high pore fluid pressure at the base of the~~
300 ~~GHSZ (i.e., the shallowest reservoir holding gas from escaping to the seafloor). Thus, seepage along the Vestnesa~~
301 ~~Ridge may have been driven by cyclic changes in stress or pore fluid pressure. Formation of tension open~~Opening
302 of fractures is facilitated if the minimum horizontal stress is smaller than the pore-fluid pressure (p_f), that is, the
303 minimum effective stress is negative ($\sigma_h' = \sigma_h - p_f < 0$) (e.g., Grauls and Baleix, 1994). ~~Secondary permeability~~
304 ~~may increase by formation of tension fractures near damaged fault zones~~ (Faulkner et al., 2010)s. A negative
305 minimum effective stress and subsequent increase in secondary permeability in a tensile stress regime can be

306 achieved particularly easy in the near-surface. Continued flow through opened faults and fractures would explain
307 brecciation and development of the observed chimneys (Fig. 2b) (e.g., Sibson, 1994).

308
309 Seepage through gas chimneys has been dominantly advective and episodic (Fig. 2; Plaza-Faverola et al., 2005)
310 due to consecutive decreases and increases in the pore fluid pressure at the base of the GHSZ in response to both,
311 regional stress field variations and also to local pressure alterations associated for example with hydrofracturing
312 (e.g., Hustoft et al., 2010 and references therein; Karstens and Berndt, 2015). A high pressure Pressure increases at
313 the base of the GHSZ in this part of the ridge is explained by a constant input of thermogenic gas from an Eocene
314 reservoir since at least ca. 2 Ma ago (Knies et al., 2018 in press).

315 —
316
317 The fact that there is not active seepage at present Along the western Vestnesa Ridge segment (i.e., being under a
318 strike-slip regime according to the models) is interesting, and somehow supports the notion that the tensile regime
319 affects the fluid flow system towards the eastern segment. The lack of seepage at present in the western segment
320 suggests that p_f at the base of the GHSZ is not high enough to overcome the minimum horizontal stress (i.e., σ_h'
321 is positive) (Fig. 32a).

323 4.4 PAST SEEPAGE – AN EFFECT OF GLACIAL STRESSES?

324 While ~~–~~ tectonic stresses are constant over short geological time spans, the chimney development and seafloor
325 seepage has been a transient process because of slight variations in pore-fluid pressure (as discussed above) or the
326 influence of other stress generating mechanisms that have repeatedly brought ~~ing~~ the system out of equilibrium.
327 Geophysical and paleontological data indicate that there was once seepage and chimney development on the
328 western Vestnesa Ridge segment (e.g., Consolaro et al., 2015; Plaza-Faverola et al., 2015; Schneider et al., 2018).

329
330 Following the same logic as for the present day seepage explanation, the negative σ_h' condition could have been
331 attained anywhere along the Vestnesa Ridge in the past due to pore fluid pressure increases at the base of the GHSZ
332 or due to a favourable orientation of the stress regime at the time.

333
334 We cannot conclusively argue about the potential effect of tensile stresses from current glacial isostasy over the
335 Vestnesa Ridge at present. However, by simple analogy with the kind of compressive stresses (magnitude and
336 orientation) reported beyond the shelf break off the mid-Norwegian margin for time spans close to present day ice

337 condition, we can sense that such an effect is minimal at present (Lund and Schmidt, 2011; Lund et al., 2009). In
338 general, it is expected that maximum glacially induced horizontal stresses (σ_H) would be dominantly oriented
339 parallel to the shelf break (Björn Lund personal communication; Lund et al., 2009). This is, dominantly N-S in the
340 area of the Vestnesa Ridge (Fig. 1). Such stress orientation would not favour opening for fluids along pre-existing
341 NW-SE oriented faults associated with seepage activity at present. It is likely, though, that the repeated waxing and
342 waning of the ice sheet caused a cyclic modulation of the stress field (varying magnitude and orientation) and
343 influenced the dynamics of gas accumulations and favourably oriented faults along the Vestnesa Ridge in the past.
344 Past glacial stresses may provide thus an alternative explanation for seepage along the entire Vestnesa Ridge extent
345 at given periods of time (Fig. 5). This scenario would be in line with the correlation between seepage and glaciation-
346 interglacial events postulated for different continental margins e.g., for chimneys off the mid-Norwegian margin
347 (Plaza-Faverola et al., 2011), the Gulf of Lion (Riboulot et al., 2014), but also along the Vestnesa Ridge (Plaza-
348 Faverola et al., 2015; Schneider et al., 2018).

349
350 The temporal variation in the stress field along the Vestnesa Ridge is also caused by its location on a constantly
351 growing plate. As the oceanic plate grows, the Vestnesa Ridge moves eastward with respect to the Molloy and
352 Knipovich Ridges, causing a westward shift in the regional stress field on the Vestnesa Ridge (Fig. 6). In the future,
353 the eastern Vestnesa Ridge may temporarily move out of the tensile zone, while the western Vestnesa Ridge moves
354 into it (Fig. 6). This suggests that a negative effective stress and subsequent active seepage may reappear at
355 pockmarks to the west of the currently active seepage zone.

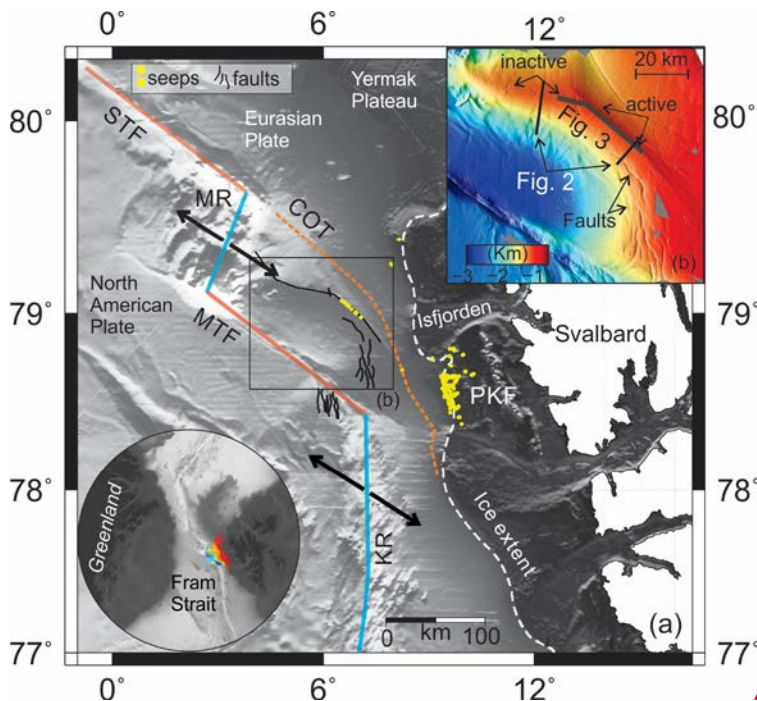
356
357 The effect of glacial stresses over the fluid flow system off west-Svalbard will be further tested (at least for the
358 Weichselian period) by implementing Lund et al., models using newly constrained Barents Sea ice-sheet models
359 (Patton et al., 2016). Additional sources of stress related to topography/bathymetry should be further investigated
360 as well to gain a comprehensive assessment of the effect of the total stress field on near-surface fluid migration in
361 the region.

365 **6- CONCLUSIONS**

366 The results of modelling the stress regime generated exclusively by mid-ocean ridge spreading in the Fram Strait
367 support seismic evidence of the correlation between faulting and seepage distribution along the Vestnesa

368 sedimentary ridge, offshore the west Svalbard margin. Tectonic stresses due to oblique spreading along the Molloy
 369 and the Knipovich ridges influences the present-present-day stress field across the west-Svalbard passive margin.
 370 A correlation between a tensile stress regimes and seepage activity suggests that episodic seepage through gas
 371 chimneys has been controlled by an interplay between varying minimum horizontal stresses and pore fluid pressure
 372 at the free gas zone beneath the gas hydrate reservoir. Our study suggests that Ppresent-day seepage is facilitated
 373 by opening of faults and fractures in a tensile stress regime or dilation on faults favourably oriented in a strike-slip
 374 regime, where pore fluid pressure overcomes the minimum horizontal stress-. Multiple seepage events along the
 375 entire extent of the Vestnesa Ridge, may have been triggered either by favourable orientation of faults with respect
 376 to mid-ocean ridge derived-stresses in the past or by additional -sources of stresses related for example to glacial
 377 isostasy. Future reactivation of currently dormant pockmarks is likely following the gradual westward propagation
 378 of the tensile stress zone on the Vestnesa Ridge as the Eurasian plate drift south-eastward.

379 **Figures**

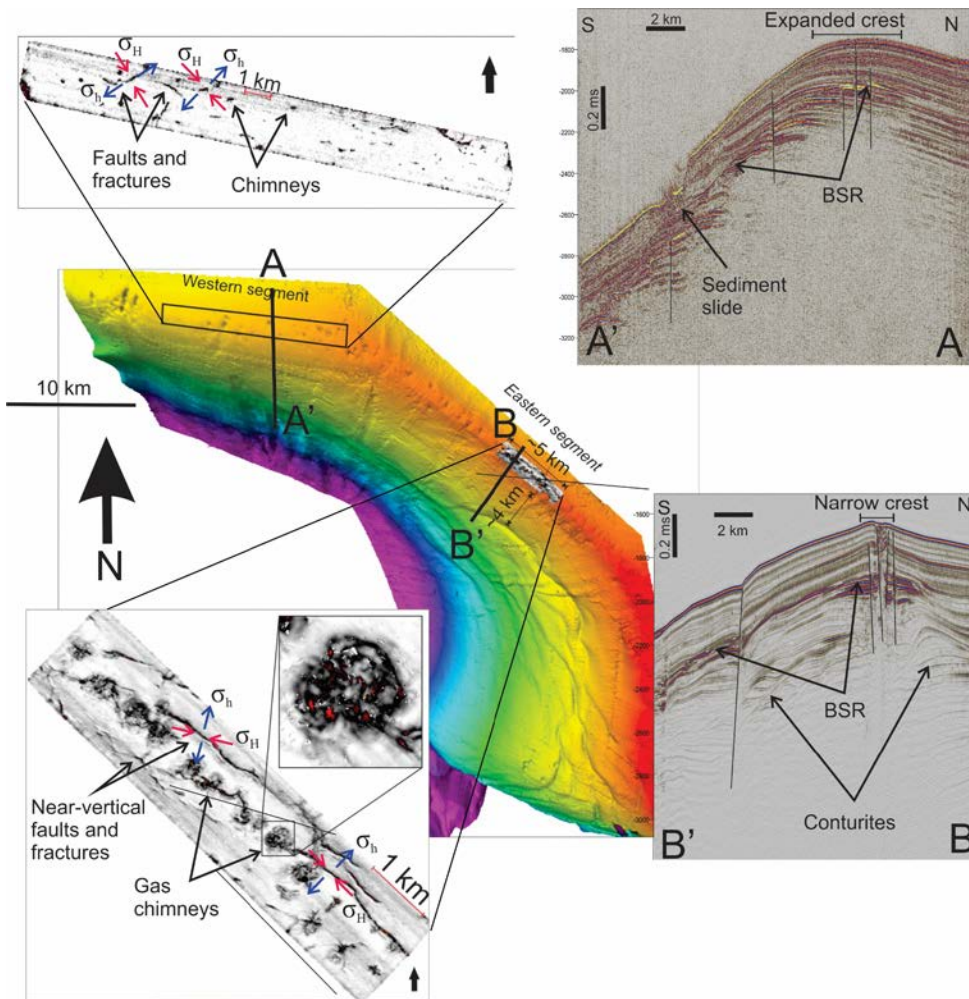


Formatted: Font: (Default) +Headings (Times New Roman), 11 pt

381 **Figure 1:** (a) International Bathymetry Chart of the Arctic Ocean (IBCAO) showing the geometry of mid-ocean
382 ridges offshore the west-Svalbard margin; (b) High resolution bathymetry along the Vestnesa Ridge (UiT, R/V HH
383 multi-beam system). Seafloor pockmarks are observed along the entire ridge but active seep sites are restricted to
384 its eastern segment; PKF=Prins Karl Foreland; STF=Spitsbergen Transform Fault; MR=Molloy Ridge;
385 MTF=Molloy Transform Fault; KR=Knipovich Ridge; COT=Continental-Oceanic Transition (Engen et al., 2008);
386 Ice-Sheet Extent (Patton et al., 2016).

387

388



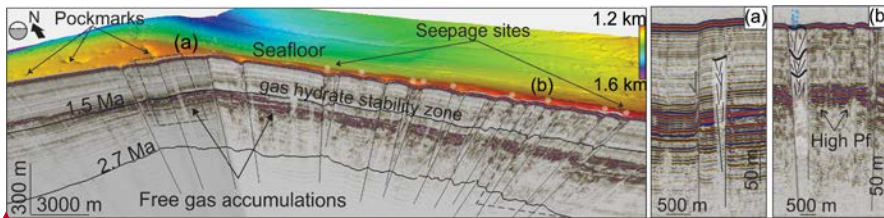
Formatted: Font: (Default) +Headings (Times New Roman), 11 pt

389
390

391 Figure 2: Composite figure with bathymetry and variance maps from 3D seismic data along the eastern and the
392 western Vestnesa Ridge segments (modified from Plaza-Faverola et al., 2015). The orientation of maximum

Formatted: Font: (Default) +Headings (Times New Roman), 11 pt

393 compressive horizontal stress (σ_H) and minimum horizontal stress (σ_h) predicted by the model are projected over
394 selected fault segments. Notice favourable orientation for opening to fluids on the eastern Vestnesa Ridge segment.
395 Two-2D seismic transects (A-A' - Bünz et al., 2012 and B-B' – Johnson et al., 2015) illustrate the morphological
396 difference of the crest of the Vestnesa Ridge (i.e., narrow vs. extended) believed to be controlled by bottom current
397 controlled deposition and erosion (Eiken and Hinz, 1993).

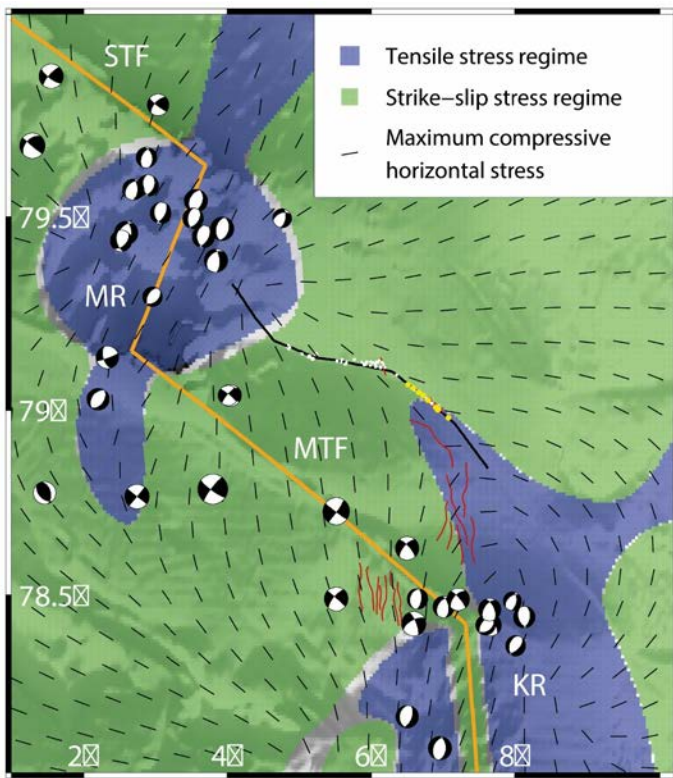


398 **Figure 32:** Integrated seismic and bathymetry image of the gas hydrate system along the Vestnesa Ridge. (a)
399 Outcropping fault located at the transition from the active to the currently inactive pockmark region; (b) Gas
400 chimneys with active seepage and inferred high pore-fluid pressure (Pf) zone.
401
402

Formatted: Font: (Default) +Headings (Times New Roman), 11 pt

Formatted: Font: (Default) +Headings (Times New Roman), 11 pt

Formatted: Font: (Default) +Headings (Times New Roman), 11 pt



403

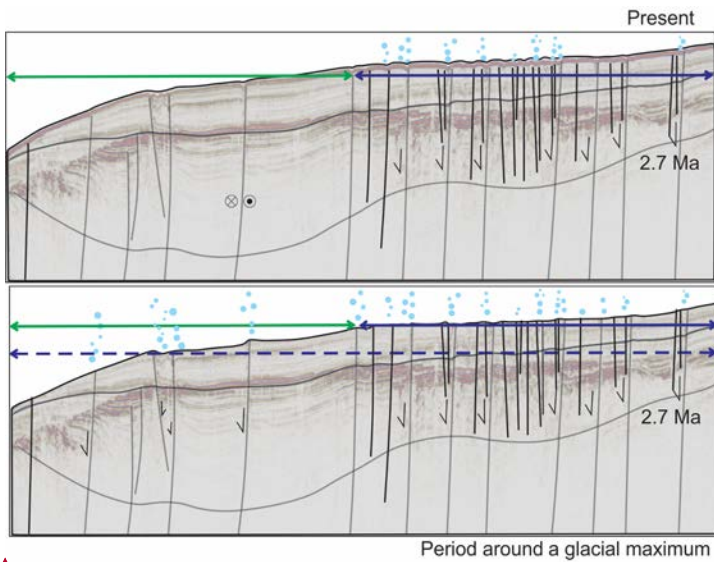
404 **Figure 43:** Modelled upper crustal tectonic stress field (blue – tensile and green - strike-slip regime) and stress
 405 orientations, due to oblique spreading at Molloy Ridge (MR) and Knipovich Ridge (KR). The seismic line is
 406 projected as reference for the crest of the Vestnesa Ridge. Red lines are faults, yellow dots seeps and white circles
 407 inactive pockmarks. The focal mechanisms are from the ISC Online Bulletin (<http://www.isc.ac.uk>).

Formatted: Font: (Default) +Headings (Times New Roman), 11 pt

Formatted: Font: (Default) +Headings (Times New Roman), 11 pt

Formatted: Font: (Default) +Headings (Times New Roman)

Formatted: Font: (Default) +Headings (Times New Roman), 11 pt

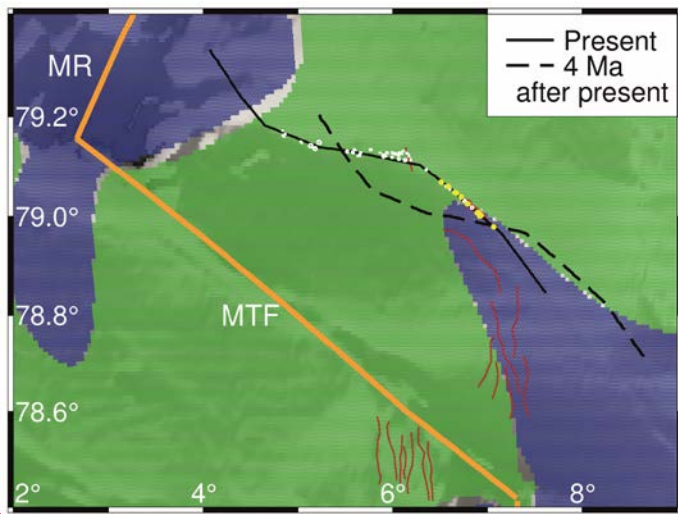


408
 409 **Figure 54:** Conceptual model of the evolution of seepage coupled to faulting and spatial variations in the stress
 410 regime (tensile=blue; strike-slip=green) along the Vestnesa Ridge, offshore the west-Svalbard margin. At present
 411 day, tensile stress from mid-ocean ridge spreading (blue solid line) favours seepage exclusively on the eastern
 412 segment of the Vestnesa Ridge. Seepage on the western Vestnesa Ridge and other regions may have been induced
 413 repeatedly since the onset of glaciations 2.7 Ma ago (Mattingsdal et al., 2014), due to tensional flexural stresses
 414 in the isostatic forebulge around the time of glacial maximums.

415
 416
 417

Formatted: Font: (Default) +Headings (Times New Roman), 11 pt

Formatted: Font: (Default) +Headings (Times New Roman), 11 pt



418
 419 **Figure 65:** Stress field in figure 3 showing the location of the Vestnesa Ridge at present and 4 Ma after present
 420 time, assuming a constant spreading velocity of 7 mm/yr in the direction N125°E. The black polygon corresponds
 421 to the seismic line in Plaza-Faverola et al., 2017 and partly shown in figure 2. It is presented as reference for the
 422 crest of the eastern and western Vestnesa Ridge segments

423
 424 **Appendix A**

425 **Model description**

426
 427 We use the analytical formulations of Okada (1985) for a finite rectangular dislocation source in elastic
 428 homogeneous isotropic half-space (Fig. A.1). The dislocation source can be used to approximate deformation along
 429 planar surfaces, such as volcanic dykes (e.g. Wright et al., 2006), sills (e.g. Pedersen and Sigmundsson, 2004),
 430 faults (e.g. Massonet et al, 1993) and spreading ridges (e.g. Keiding et al., 2009). More than one dislocations can
 431 be combined to obtain more complex geometry of the source or varying deformation along a planar source. The
 432 deformation of the source can be defined as either lateral shear (strike-slip for faults), vertical shear (dip-slip at
 433 faults) or tensile opening.

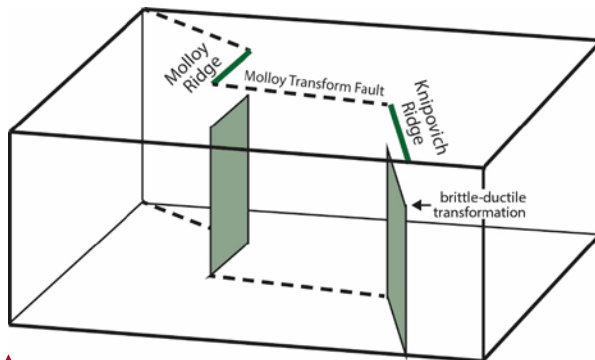
Formatted: Font: (Default) +Headings (Times New Roman), 11 pt

Formatted: Font: (Default) +Headings (Times New Roman), 11 pt

Formatted: Font: (Default) +Headings (Times New Roman), 11 pt

435 The Okada model assumes flat Earth without inhomogeneities. While the flat-earth assumption is usually adequate
 436 for regional studies (e.g. Wolf, 1984), the lateral inhomogeneities can sometimes cause considerable effect on the
 437 deformation field (e.g. Okada, 1985). However, the dislocation model is useful as a first approximation to the
 438 problem.

439
 440 At mid-ocean ridges, deformation is driven by the continuous spreading caused primarily by gravitational stress
 441 due to the elevation of the ridges, but also basal drag and possibly slab pull. Deformation occurs continuously in
 442 the ductile part of the crust. Meanwhile, elastic strain builds in the upper, brittle part of the crust. To model this
 443 setting, the upper boundary of the dislocation source must be located at the depth of the brittle-ductile transition
 444 zone. The lower boundary of the source is set to some arbitrary large depth to avoid boundary effects.



446
 447 **Fig A.1** Extract of model showing the location of the dislocation sources (light green) for Molloy and
 448 **Knipovich ridges**. Note that the model is an infinite half-space, i.e. it has no lateral or lower boundary.

449
 450 The Okada model provides the displacements u_x, u_y, u_z (or velocities if deformation is time-dependent) at defined
 451 grid points at the surface and subsurface. It also provides strain (or strain rates) defined as:

$$\epsilon_{ij} = \frac{1}{2}(u_{i,j} + u_{j,i})$$

452
 453 The stress field can then be calculated from the predicted strain rates. In homogeneous isotropic media, stress is
 454 related to strain as:

$$\sigma_{ij} = \lambda \delta_{ij} \epsilon_{kk} + 2\mu \epsilon_{ij}$$

Formatted: Font: (Default) +Headings (Times New Roman), 11 pt

Formatted: Font: (Default) +Headings (Times New Roman), 11 pt

Formatted: Font: (Default) +Headings (Times New Roman), 11 pt

Formatted: Font: (Default) +Headings (Times New Roman), 11 pt

Formatted: Font: (Default) +Headings (Times New Roman), 11 pt

Formatted: Font: (Default) +Headings (Times New Roman), 11 pt

Formatted: Font: (Default) +Headings (Times New Roman), 11 pt

Formatted: Font: (Default) +Headings (Times New Roman), 11 pt

Formatted: Font: 11 pt

Formatted: Font: 11 pt

Formatted: Font: 11 pt

Formatted: Font: 11 pt

Formatted: Font: (Default) +Headings (Times New Roman), 11 pt

Formatted: Font: 11 pt

Formatted: Font: 11 pt

Formatted: Font: (Default) +Headings (Times New Roman), 11 pt

456 where δ_{ij} is the Kronecker delta, λ is Lamé's first parameter, and μ is the shear modulus. Lamé's first parameter
457 does not have a physical meaning but is related to the shear modulus and Poisson's ratio (ν) as $\lambda = \frac{2\mu\nu}{1-2\nu}$.
458 The absolute values of stress are in general difficult to model (e.g. Hergert and Heidbach, 2011), and not possible
459 with our analytical model. However, the model provides us with the orientations and relative magnitude of the
460 stresses. That is, we know the relative magnitudes of the vertical stress (σ_v), maximum horizontal stress (σ_H) and
461 minimum horizontal stress (σ_h). From this, the stress regime can be defined as either tensile ($\sigma_v > \sigma_H > \sigma_h$), strike-
462 slip ($\sigma_H > \sigma_v > \sigma_h$) or compressive ($\sigma_H > \sigma_h > \sigma_v$).

463 **Author contribution**

464 Andrea Plaza-Faverola conceived the paper idea. She is responsible for seismic data processing and interpretation.
465 Marie Keiding did the tectonic modelling. The paper is the result of integrated work between both.

466 **ACKNOWLEDGEMENTS**

467 This research is part of the Centre for Arctic Gas Hydrate, Environment and Climate (CAGE) supported by the
468 Research Council of Norway through its Centres of Excellence funding scheme grant No. 223259. Marie Keiding
469 is supported by the NEONOR2 project at the Geological Survey of Norway. Special thanks to Björn Lund, Peter
470 Schmidt, Henry Patton, and Alun Hubbard for their interest in the present project and constructive discussions
471 about isostasy and glacial stresses. We are thankful to various reviewers that have contributed to the improvement
472 of the manuscript. Seismic data is archived at CAGE – Centre for Arctic Gas Hydrate, Environment and Climate,
473 Tromsø, Norway and can be made available by contacting APF. Modelled stresses can be made available by
474 contacting MK.

475 **References:**

476 Ambrose, W.G., Panieri, G., Schneider, A., Plaza-Faverola, A., Carroll, M.L., Åström, E.K., Locke, W.L., Carroll, J.,
477 2015. Bivalve shell horizons in seafloor pockmarks of the last glacial-interglacial transition: a thousand years of
478 methane emissions in the Arctic Ocean. Geochemistry, Geophysics, Geosystems 16, 4108-4129.
479 Andreassen, K., Hubbard, A., Winsborrow, M., Patton, H., Vadakkepuliambatta, S., Plaza-Faverola, A.,
480 Gudlaugsson, E., Serov, P., Deryabin, A., Mattingsdal, R., 2017. Massive blow-out craters formed by hydrate-
481 controlled methane expulsion from the Arctic seafloor. Science 356, 948-953.
482 Bünz, S., Polyakov, S., Vadakkepuliambatta, S., Consolaro, C., Mienert, J., 2012. Active gas venting through
483 hydrate-bearing sediments on the Vestnesa Ridge, offshore W-Svalbard. Marine geology.

Formatted: Font: (Default) +Headings (Times New Roman), 11 pt

Formatted: Font: (Default) +Headings (Times New Roman), 11 pt

Formatted: Font: (Default) +Headings (Times New Roman), 11 pt

Formatted: Font: (Default) +Headings (Times New Roman), 11 pt

Formatted: Font: (Default) +Headings (Times New Roman), 11 pt

Formatted: Font: (Default) +Headings (Times New Roman), 11 pt

Formatted: Font: (Default) +Headings (Times New Roman), 11 pt

Formatted: Font: (Default) +Headings (Times New Roman), 11 pt

Formatted: Font: (Default) +Headings (Times New Roman), 11 pt

Formatted

Formatted

Formatted

Formatted

Formatted

Formatted

Formatted

Formatted

Formatted

Formatted

Formatted

Formatted

Formatted

Formatted

Formatted: Font: (Default) +Headings (Times New Roman)

487 Consolaro, C., Rasmussen, T., Panieri, G., Mienert, J., Bünz, S., Szybor, K., 2015. Carbon isotope ($\delta^{13}\text{C}$)
488 excursions suggest times of major methane release during the last 14 kyr in Fram Strait, the deep-water
489 gateway to the Arctic. *Climate of the Past* 11, 669-685.

490 Crane, K., Doss, H., Vogt, P., Sundvor, E., Cherkashov, G., Poroshina, I., Joseph, D., 2001. The role of the
491 Spitsbergen shear zone in determining morphology, segmentation and evolution of the Knipovich Ridge. *Marine*
492 *geophysical researches* 22, 153-205.

493 Crane, K., Sundvor, E., Buck, R., Martinez, F., 1991. Rifting in the northern Norwegian-Greenland Sea: Thermal
494 tests of asymmetric spreading. *Journal of Geophysical Research: Solid Earth* 96, 14529-14550.

495 DeMets, C., Gordon, R.G., Argus, D.F., 2010. Geologically current plate motions. *Geophysical Journal*
496 *International* 181, 1-80.

497 Dickens, G.R., 2011. Down the rabbit hole: Toward appropriate discussion of methane release from gas hydrate
498 systems during the Paleocene-Eocene thermal maximum and other past hyperthermal events. *Climate of the*
499 *Past* 7, 831-846.

500 Ehlers, B.-M., Jokat, W., 2009. Subsidence and crustal roughness of ultra-slow spreading ridges in the northern
501 North Atlantic and the Arctic Ocean. *Geophysical Journal International* 177, 451-462.

502 Eiken, O., Hinz, K., 1993. Contourites in the Fram Strait. *Sedimentary Geology* 82, 15-32.

503 Eldholm, O., Faleide, J.I., Myhre, A.M., 1987. Continent-ocean transition at the western Barents Sea/Svalbard
504 continental margin. *Geology* 15, 1118-1122.

505 Engen, Ø., Faleide, J.I., Dyreng, T.K., 2008. Opening of the Fram Strait gateway: A review of plate tectonic
506 constraints. *Tectonophysics* 450, 51-69.

507 Faleide, J., Gudlaugsson, S., Eldholm, O., Myhre, A., Jackson, H., 1991. Deep seismic transects across the sheared
508 western Barents Sea-Svalbard continental margin. *Tectonophysics* 189, 73-89.

509 Faleide, J.I., Solheim, A., Fiedler, A., Hjelstuen, B.O., Andersen, E.S., Vanneste, K., 1996. Late Cenozoic evolution
510 of the western Barents Sea-Svalbard continental margin. *Global and Planetary Change* 12, 53-74.

511 Faulkner, D., Jackson, C., Lunn, R., Schlische, R., Shipton, Z., Wibberley, C., Withjack, M., 2010. A review of
512 recent developments concerning the structure, mechanics and fluid flow properties of fault zones. *Journal of*
513 *Structural Geology* 32, 1557-1575.

514 Fjeldskaar, W., Amantov, A., 2017. Effects of glaciations on sedimentary basins. *Journal of Geodynamics*.

515 Gaina, C., Nikishin, A., Petrov, E., 2015. Ultraslow spreading, ridge relocation and compressional events in the
516 East Arctic region: A link to the Eureka orogeny? *arktos* 1, 16.

517 Geersen, J., Scholz, F., Linke, P., Schmidt, M., Lange, D., Behrmann, J.H., Völker, D., Hensen, C., 2016. Fault zone
518 controlled seafloor methane seepage in the rupture area of the 2010 Maule Earthquake, Central Chile.
519 *Geochemistry, Geophysics, Geosystems* 17, 4802-4813.

520 Grauls, D., Baleix, J., 1994. Role of overpressures and in situ stresses in fault-controlled hydrocarbon migration:
521 A case study. *Marine and Petroleum Geology* 11, 734-742.

522 Heidbach, O., Tingay, M., Barth, A., Reinecker, J., Kurfeß, D., Müller, B., 2010. Global crustal stress pattern based
523 on the World Stress Map database release 2008. *Tectonophysics* 482, 3-15.

524 Hillis, R.R., 2001. Coupled changes in pore pressure and stress in oil fields and sedimentary basins. *Petroleum*
525 *Geoscience* 7, 419-425.

526 Hunter, S., Goldobin, D., Haywood, A., Ridgwell, A., Rees, J., 2013. Sensitivity of the global submarine hydrate
527 inventory to scenarios of future climate change. *Earth and Planetary Science Letters* 367, 105-115.

528 Hustoft, S., Bunz, S., Mienert, J., Chand, S., 2009. Gas hydrate reservoir and active methane-venting province in
529 sediments on < 20 Ma young oceanic crust in the Fram Strait, offshore NW-Svalbard. *Earth and Planetary*
530 *Science Letters* 284, 12-24.

531 Hustoft, S., Bünz, S., Mienert, J., 2010. Three-dimensional seismic analysis of the morphology and spatial
532 distribution of chimneys beneath the Nyegga pockmark field, offshore mid-Norway. *Basin Research* 22, 465-
533 480.

534 Jakobsson, M., Backman, J., Rudels, B., Nycander, J., Frank, M., Mayer, L., Jokat, W., Sangiorgi, F., O'Regan, M.,
535 Brinkhuis, H., 2007. The early Miocene onset of a ventilated circulation regime in the Arctic Ocean. *Nature* 447,
536 986-990.

537 Jansen, E., Sjøholm, J., 1991. Reconstruction of glaciation over the past 6 Myr from ice-borne deposits in the
538 Norwegian Sea. *Nature* 349, 600.

539 Jansen, E., Sjøholm, J., Bleil, U., Erichsen, J., 1990. Neogene and Pleistocene glaciations in the northern
540 hemisphere and late Miocene—Pliocene global ice volume fluctuations: Evidence from the Norwegian Sea,
541 *Geological History of the Polar Oceans: Arctic versus Antarctic*. Springer, pp. 677-705.

542 Johnson, J.E., Mienert, J., Plaza-Faverola, A., Vadakkepuliambatta, S., Knies, J., Bünz, S., Andreassen, K., Ferré,
543 B., 2015. Abiotic methane from ultraslow-spreading ridges can charge Arctic gas hydrates. *Geology*, G36440.
544 36441.

545 Judd, A., Hovland, M., 2009. *Seabed fluid flow: the impact on geology, biology and the marine environment*.
546 Cambridge University Press.

547 Jung, N.-H., Han, W.S., Watson, Z., Graham, J.P., Kim, K.-Y., 2014. Fault-controlled CO₂ leakage from natural
548 reservoirs in the Colorado Plateau, East-Central Utah. *Earth and Planetary Science Letters* 403, 358-367.

549 Karstens, J., Berndt, C., 2015. Seismic chimneys in the Southern Viking Graben—Implications for palaeo fluid
550 migration and overpressure evolution. *Earth and Planetary Science Letters* 412, 88-100.

551 Keiding, M., Lund, B., Árnadóttir, T., 2009. Earthquakes, stress, and strain along an obliquely divergent plate
552 boundary: Reykjanes Peninsula, southwest Iceland. *Journal of Geophysical Research: Solid Earth* 114.

553 Knies, J., Daszinnies, M., Plaza-Faverola, A., Chand, S., Sylta, Ø., Bünz, S., Johnson, J.E., Mattingsdal, R., Mienert,
554 J., 2018. Modelling persistent methane seepage offshore western Svalbard since early Pleistocene. *Marine and*
555 *Petroleum Geology* 91, 800-811.

556 Knies, J., Matthiessen, J., Vogt, C., Laberg, J.S., Hjelstuen, B.O., Smelror, M., Larsen, E., Andreassen, K., Eidvin, T.,
557 Vorren, T.O., 2009. The Plio-Pleistocene glaciation of the Barents Sea–Svalbard region: a new model based on
558 revised chronostratigraphy. *Quaternary Science Reviews* 28, 812-829.

559 Lund, B., Schmidt, P., 2011. Stress evolution and fault stability at Olkiluoto during the Weichselian glaciation.
560 Posiva Oy.

561 Lund, B., Schmidt, P., Hieronymus, C., 2009. Stress evolution and fault stability during the Weichselian glacial
562 cycle. Swedish Nuclear Fuel and Waste Management Co, Stockholm, Sweden.

563 Lund, B., Townend, J., 2007. Calculating horizontal stress orientations with full or partial knowledge of the
564 tectonic stress tensor. *Geophysical Journal International* 170, 1328-1335.

565 Mattingsdal, R., Knies, J., Andreassen, K., Fabian, K., Husum, K., Grøsfjeld, K., De Schepper, S., 2014. A new 6
566 Myr stratigraphic framework for the Atlantic–Arctic Gateway. *Quaternary Science Reviews* 92, 170-178.

567 Morgan, W.J., 1981. 13. Hotspot tracks and the opening of the Atlantic and Indian Oceans. *The oceanic*
568 *lithosphere* 7, 443.

569 Myhre, A.M., Eldholm, O., 1988. The western Svalbard margin (74–80 N). *Marine and Petroleum Geology* 5, 134-
570 156.

571 Nasuti, A., Olesen, O., 2014. Chapter 4: Magnetic data. In: Hopper J.R., Funck T., Stoker T., Arting U., Peron-
572 Pinvidic G., Doornebal H. & Gaina C. (eds) Tectonostratigraphic Atlas of the North-East Atlantic Region.
573 Geological Survey of Denmark and Greenland (GEUS), Copenhagen, Denmark, 41–51. .
574 Okada, Y., 1985. Surface deformation due to shear and tensile faults in a half-space. Bulletin of the
575 seismological society of America 75, 1135-1154.
576 Patton, H., Hubbard, A., Andreassen, K., Winsborrow, M., Stroeven, A.P., 2016. The build-up, configuration, and
577 dynamical sensitivity of the Eurasian ice-sheet complex to Late Weichselian climatic and oceanic forcing.
578 Quaternary Science Reviews 153, 97-121.
579 Petersen, C.J., Bünz, S., Hustoft, S., Mienert, J., Klaeschen, D., 2010. High-resolution P-Cable 3D seismic imaging
580 of gas chimney structures in gas hydrated sediments of an Arctic sediment drift. Marine and Petroleum Geology
581 doi: 10.1016/j.marpetgeo.2010.06.006, 1-14.
582 Planke, S., Eriksen, F.N., Berndt, C., Mienert, J., Masson, D., 2009. P-Cable high-resolution seismic.
583 Oceanography 22, 85.
584 Plaza-Faverola, A., Bünz, S., Mienert, J., 2011. Repeated fluid expulsion through sub-seabed chimneys offshore
585 Norway in response to glacial cycles. Earth and Planetary Science Letters 305, 297-308.
586 Plaza-Faverola, A., Bünz, S., Johnson, J.E., Chand, S., Knies, J., Mienert, J., Franek, P., 2015. Role of tectonic
587 stress in seepage evolution along the gas hydrate-charged Vestnesa Ridge, Fram Strait. Geophysical Research
588 Letters 42, 733-742.
589 Plaza-Faverola, A., Henrys, S., Pecher, I., Wallace, L., Klaeschen, D., 2016. Splay fault branching from the
590 Hikurangi subduction shear zone: Implications for slow slip and fluid flow. Geochemistry, Geophysics,
591 Geosystems 17, 5009-5023.
592 Plaza-Faverola, A., Vadakkepuliymbatta, S., Hong, W.L., Mienert, J., Bünz, S., Chand, S., Greinert, J., 2017.
593 Bottom-simulating reflector dynamics at Arctic thermogenic gas provinces: an example from Vestnesa Ridge,
594 offshore west-Svalbard. Journal of Geophysical Research: Solid Earth.
595 Portnov, A., Vadakkepuliymbatta, S., Mienert, J., Hubbard, A., 2016. Ice-sheet-driven methane storage and
596 release in the Arctic. Nature communications 7.
597 Riboulot, V., Thomas, Y., Berné, S., Jouet, G., Cattaneo, A., 2014. Control of Quaternary sea-level changes on gas
598 seeps. Geophysical Research Letters 41, 4970-4977.
599 Roy, S., Senger, K., Braathen, A., Noormets, R., Hovland, M., Olausen, S., 2014. Fluid migration pathways to
600 seafloor seepage in inner Isfjorden and Adventfjorden, Svalbard. Geological controls on fluid flow and seepage
601 in western Svalbard fjords, Norway. An integrated marine acoustic study.
602 Schiffer, C., Tegner, C., Schaeffer, A.J., Pease, V., Nielsen, S.B., 2018. High Arctic geopotential stress field and
603 implications for geodynamic evolution. Geological Society, London, Special Publications 460, 441-465.
604 Schneider, A., Panieri, G., Lepland, A., Consolaro, C., Crémière, A., Forwick, M., Johnson, J.E., Plaza-Faverola, A.,
605 Sauer, S., Knies, J., 2018. Methane seepage at Vestnesa Ridge (NW Svalbard) since the Last Glacial Maximum.
606 Quaternary Science Reviews 193, 98-117.
607 Sibson, R.H., 1994. Crustal stress, faulting and fluid flow. Geological Society, London, Special Publications 78, 69-
608 84.
609 Skarke, A., Ruppel, C., Kodis, M., Brothers, D., Lobecker, E., 2014. Widespread methane leakage from the sea
610 floor on the northern US Atlantic margin. Nature Geoscience 7, 657-661.
611 Smith, A.J., Mienert, J., Bünz, S., Greinert, J., 2014. Thermogenic methane injection via bubble transport into the
612 upper Arctic Ocean from the hydrate-charged Vestnesa Ridge, Svalbard. Geochemistry, Geophysics,
613 Geosystems.

614 Steffen, H., Kaufmann, G., Wu, P., 2006. Three-dimensional finite-element modeling of the glacial isostatic
615 adjustment in Fennoscandia. *Earth and Planetary Science Letters* 250, 358-375.

616 Svensen, H., Planke, S., Møller, S., Jamveit, B., Myklebust, R., Eidem, T.R., Rey, S.S., 2004. Release of
617 methane from a volcanic basin as a mechanism for initial Eocene global warming. *Nature* 429, 542-545.

618 Turcotte, D.L., Schubert, G., 2002. *Geodynamics*. Cambridge University Press.

619 Vanneste, M., Guidard, S., Mienert, J., 2005. Arctic gas hydrate provinces along the western Svalbard
620 continental margin. *Norwegian Petroleum Society Special Publications* 12, 271-284.

621 Vogt, P.R., Crane, K., Sundvor, E., Max, M.D., Pfirman, S.L., 1994. Methane-generated (?) pockmarks on young,
622 thickly sedimented oceanic crust in the Arctic: Vestnesa ridge, Fram strait. *Geology* 22, 255-258.

623 Wallmann, K., Riedel, M., Hong, W., Patton, H., Hubbard, A., Pape, T., Hsu, C., Schmidt, C., Johnson, J., Torres,
624 M., 2018. Gas hydrate dissociation off Svalbard induced by isostatic rebound rather than global warming.
625 *Nature communications* 9, 83.

626 Westbrook, G.K., Thatcher, K.E., Rohling, E.J., Piotrowski, A.M., Palike, H., Osborne, A.H., Nisbet, E.G., Minshull,
627 T.A., Lanoiselle, M., James, R.H., Hühnerbach, V., Green, D., Fisher, R.E., Crocker, A.J., Chabert, A., Bolton, C.,
628 Beszczynska-Møller, A., Berndt, C., Aquilina, A., 2009. Escape of methane gas from the seabed along the West
629 Spitsbergen continental margin. *Geophysical Research Letters* 36, 5.

630 Zoback, M.D., Zoback, M.L., 2002. 34 State of stress in the Earth's lithosphere. *International Geophysics* 81, 559-
631 XII.

632